

OUTAGE PERFORMANCE OPTIMIZATION FOR TWO-WAY RELAY-AIDED COOPERATIVE NOMA WITH SWIPT

Nguyễn Như Thắng, Ngô Thanh Tùng*

Trường Đại học Thông tin Liên lạc

Thông tin chung:

Ngày nhận bài: 11/05/2024

Ngày phản biện: 12/05/2024

Ngày duyệt đăng:

30/05/2024

*Tác giả liên hệ:

tungngo thanh77@gmail.com

Title:

Tối ưu xác suất dừng cho hệ thống NOMA hợp tác có trợ giúp chuyển tiếp hai chiều với SWIPT.

Từ khóa:

Đa truy nhập không trực giao (NOMA), Truyền thông tin và năng lượng đồng thời (SWIPT), Xác suất dừng (OP)

Keywords:

Non-orthogonal multiple access (NOMA), Simultaneous wireless information and power transfer (SWIPT), Outage Probability (OP)

TÓM TẮT: Bài báo này, đề xuất hệ thống truyền thông đa truy cập không trực giao (NOMA: Non-orthogonal multiple access) chuyển tiếp hai chiều (TWR: two-way relay) nhằm cải thiện hiệu quả phổ tần. Sử dụng kỹ thuật biến đổi thông tin và năng lượng đồng thời (SWIPT: simultaneous wireless information and power transfer) để nâng cao hiệu quả sử dụng năng lượng. Để đánh giá phẩm chất hệ thống, chúng tôi tính toán biểu thức xác suất dừng hoạt động trong ba pha liên lạc ở kênh truyền Rayleigh fading. Để giải quyết bài toán tối ưu, thuật toán lập được sử dụng. Thông qua các kết quả mô phỏng và tính toán chỉ ra rằng mô hình đề xuất có hiệu quả sử dụng phổ tần và năng lượng cao hơn các hệ thống truyền thống.

ABSTRACT: In this paper, we aim to enhance spectrum efficiency in infrastructure-based Non-Orthogonal Multiple Access (NOMA) networks over Rayleigh fading channels. To achieve this, we introduce a Simultaneous Wireless Information and Power Transfer (SWIPT)-enabled Two-Way Relay (TWR) system. We then derive closed-form expressions for the outage probability for both near and far users in three-time slots. We design an iterative algorithm to solve this optimization problem efficiently. Finally, through numerical simulations, we demonstrate that our proposed scheme outperforms baseline benchmarks, confirming the effectiveness of our approach.

1. Introduction

With the rapid evolution of smart devices, wireless communication has become more prevalent. Unfortunately, the limited spectrum makes it difficult to accommodate the increasing number of devices and deliver the best possible service [1]. One that solution can address these issues is the utilization of On the other hand, with the progress of the radio frequency (RF) energy harvesting technique, simultaneous wireless information and power transfer (SWIPT) is considered a promising technology to

provide energy for relays to make them sustainable [2]. The above kinds of literature are mainly focused on the performances of one-way relay (OWR)-aided SWIPT-NOMA networks. In such networks, the data are transmitted from source to relay and then to the destinations. In actuality, two-way relay (TWR) communications can improve the spectrum effectively.

A TWR-assisted cooperative CNOMA network is proposed where the spectral efficiency is enhanced [3]. In an infrastructure-based NOMA network, a TWR with analog network coding is employed to

complete information exchange between the users and the base station. As an enhancement of TWR system, a SWIPT-enabled secondary user is served as a TWR in the cognitive radio (CR) network [4]. Three-phase transmission scheme with a fixed power distribution factor and time distribution factor designed in [5].

When related to NOMA transmission, two SWIPT-enabled TWRs with the source forming a NOMA pair to extend the coverage of the far users in [6]. Furthermore, to enhance the energy harvesting efficiency in a multiple-input single-output (MISO) full-duplex TWR-NOMA system, a bilevel programming (BLP) based method is proposed in [7].

Differently, in another FD TWR network with PS protocol over Nakagami-m fading channels, the outage performance under imperfect channel state information (CSI) with hardware impairments is studied in [8]. In [9], the authors design a two-phase transmission scheme based on TWRs in a network where the signal composed based on NOMA transmission. In the proposed scheme, the signal is transmitted to multiple relays in the first slot and transmitted to the terminal node in the second slot, through which the performance is improved compared to the conventional TWR method.

Based on the current research, we manifest that SWIPT-enabled NOMA network with either HD or FD OWR can gain a better performance such as outage probability, system throughput, BER, energy efficiency or data rate compared with that in the Orthogonal Multiple Access (OMA) network. Some endeavors have been concerned with fulfilling the data transmission between a pair of primary users in CR or between two nodes in a wireless network via traditional TWR. Other works have also been devoted to analyzing the performance of the SWIPT-enabled TWR network with hardware impairments, residual self-interference, and a non-linear power amplifier. Other works have also been

devoted to proposing a SWIPT-enabled TWR network to enlarge coverage, enhancing energy harvesting efficiency and system performance.

However, in the aforementioned literatures, the data exchange between near and far user by the collaboration of a SWIPT-enabled TWR and base station (BS) in the infrastructure based NOMA network has not been leveraged yet. To fill this gap is the main objective of this paper. In order to finish the information exchange between near and far user in the infrastructure based NOMA network, we propose a TWR-aided SWIPT-NOMA network with the aim of combining TWR with SWIPT to enhance energy efficiency, then we design a hybrid protocol in the system. Also, we explore the optimal value to achieve a lower system outage probability. The contributions of this paper are as follows:

i) We import a SWIPT-enabled TWR to the infrastructure-based NOMA network over Rayleigh fading channels. Then we propose a three-phase data exchange scheme based on a hybrid relaying protocol combining PS with TS protocol (HPTSR). We derive the closed expressions of outage probability for the near user and the far user, respectively. ii) We construct an optimization problem to minimize the system outage probability under the constraints of the power allocation factor and time allocation factor. The optimization problem with Bessel functions is solved by an iterative algorithm. iii) Simulation results show the superiority of our proposed design in terms of system outage probability compared with baseline schemes. The baseline schemes include the SWIPT-enabled TWR CR network and the SWIPT-enabled TWR with a direct link with fixed power and time allocation factor, respectively, also the TWR-aided NOMA without SWIPT.

The remainder of this paper is organized as follows. In Section 2, we introduce the system model. We derive the closed expressions of outage probability for the near user and the far user in Section 3. Problem

formulation and solution to the optimization problem are presented in Section 4. Then we present simulation results and conclusion in Sections 5 and 6, respectively.

2. Theoretical framework and methods

As shown in Figure 1, the system in this paper contains a source node S, a TWR R and two users, denoted as UE1 and UE2. All users are equipped with a single antenna. It is assumed that the link between UE2 and the source node does not exist due to deep fading or shadowing, so does the link between UE1 and UE2. UE2 is far from the base station and exchanges data with the source node through R. $h_i \sim CN(0, \lambda_i)$ ($i=1,2,3,4,5,6$) denotes the Rayleigh fading channel.

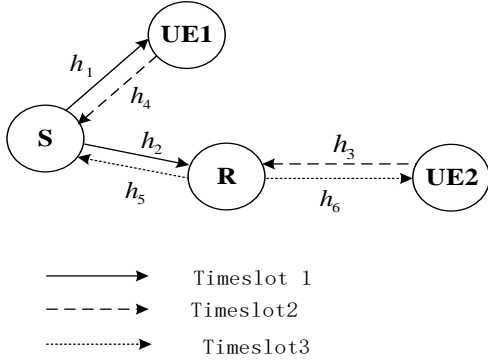


Figure 1. System model

The distance between S and UE1, S and R, R and UE2 is denoted by d_1, d_2, d_3 , respectively. It is assumed that R obtains energy from the RF signal and forward the data based on DF protocol.

The three-stage hybrid protocol is shown in Figure 2. It is assumed that the transmit time is T. The entire duration T is initially divided into three time slots, with each of duration being θT and $(1-2\theta)T$ respectively, where $\theta(0 < \theta < 1)$ is the time switching factor. Within the first timeslot θT , the relay R takes energy from the signal transmitted by the source node. The power received from the source node is divided into two parts, βP_s is used for energy harvesting and the rest $(1-\beta)P_s$ is used for information decoding, where P_s is the transmit power and

$\beta(0 < \beta < 1)$ is the power allocation factor. In the second timeslot, UE1 transmits a signal to the source node to complete the two-way information exchange. At the same time, UE2 transmits a signal to the relay R. R obtains a portion of the power βP_2 of the signal from UE2 for energy harvesting and the rest $(1-\beta)P_2$ for information decoding, where P_2 is the transmit power of UE2. Within the third timeslot of duration $(1-2\theta)T$, R mixes the two information streams received from UE2 and S and then uses the harvested energy to broadcast the encoded information to both S and UE2. Once S and UE2 receive the broadcasted information from R, they can decode the required information from the mixed information based on their priori experience.

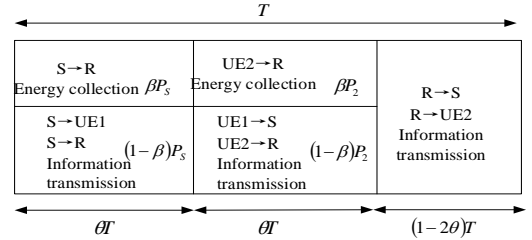


Figure 2. Hybrid Relay Protocol

In the first time slot, the source node S transmits signal x to R and UE2 based on NOMA technique, $x = \sqrt{a_1 P_s} x_1 + \sqrt{a_2 P_s} x_2$, where a_1 and a_2 denotes the NOMA power distribution coefficient per unit power RF signal x_1 and x_2 , respectively, $a_1 + a_2 = 1, a_2 > a_1$. The signals received by R and UE1 can be expressed by:

$$y_R^1 = \sqrt{\frac{P_s}{d_2^m}} h_2 (\sqrt{a_1} x_1 + \sqrt{a_2} x_2) + n_R \quad (1)$$

$$y_1^1 = \sqrt{\frac{P_s}{d_1^m}} h_1 (\sqrt{a_1} x_1 + \sqrt{a_2} x_2) + n_1 \quad (2)$$

Where $n_c, \sim CN(0, N_0)$ is the additive Gaussian white noise of the receiving antenna at node R, m is the path loss index. The superscript 1 indicates at the first time slot.

Since $a_2 > a_1$, UE1 and R use serial interference cancellation to treat low-power signals x_1 as noise, and decode high-power

signals x_2 . After successful decoding x_2 , x_2 are removed from the received mixed signal, and then the low-power signals x_1 are decoded to enable multi-user signal detection. The SNR of the UE1 decoded signal x_2 is:

$$\gamma_{UE1,x2} = \frac{P_S d_1^{-m} |h_1|^2 a_2}{P_S d_1^{-m} |h_1|^2 a_2 + N_0} \quad (3)$$

Let $\rho_S = P_S / N_0$ the above equation can be expressed by:

$$\gamma_{UE1,x2} = \frac{\rho_S |h_1|^2 a_1}{\rho_S |h_1|^2 a_1 + d_1^m} \quad (4)$$

UE1 successfully decodes the signal x_2 and removes it before decoding x_1 , the SNR of UE1 for decoding x_1 is

$$\gamma_{UE1,x1} = \rho_S |h_1|^2 a_1 / d_1^m \quad (5)$$

The TWR based on the hybrid protocol performs information decoding and energy collection of the received signal. The energy collected by the relay in the first time slot is expressed as:

$$E_1 = \eta \beta P_S |h_2|^2 \theta T / d_2^m \quad (6)$$

where $\eta (0 < \eta < 1)$ is the energy conversion efficiency of the RF signal into energy.

The decoded and transmitted signals from the relay node can be expressed as

$$\sqrt{1-\beta} y_R^1 = \sqrt{\frac{(1-\beta)P_S}{d_2^m}} h_2 (\sqrt{a_1} x_1 + \sqrt{a_2} x_2) + \sqrt{1-\beta} n_R + n_c \quad (7)$$

where n_c is the additive Gaussian white noise at the receiving antenna of the relay node.

The SNR for R decoding signal x_2 can be expressed as:

$$\gamma_{R,x2} = \frac{(1-\beta)a_2\rho_S|h_2|^2}{(1-\beta)a_1\rho_S|h_2|^2+d_2^m} \quad (8)$$

In the second time slot, UE2 transmits a signal x_{2U} to the relay. At the same time, UE1 transmits a signal x_{1U} to the base station to complete the information exchange between

the base station and UE1. The received signal at R is given by:

$$y_R^2 = \sqrt{\frac{P_2}{d_3^m}} h_2 x_{2U} + n_R \quad (9)$$

Where P_2 is the transmit power of UE2.

The energy collected by R from the received signal can be denoted by:

$$E_2 = \frac{\eta \beta P_2 |h_3|^2}{d_3^m} \theta T \quad (10)$$

The SNR for the relay decoding x_{2U} can be denoted by:

$$\gamma_{R,x2U} = (1-\beta)\rho_2|h_3|^2/d_3^m \quad (11)$$

The signal received by the source node S from UE1 is

$$y_S^2 = \sqrt{\frac{P_1}{d_1^m}} h_4 x_{1U} + n_S \quad (12)$$

The SNR for S decoding x_{1U} is

$$\gamma_{S,x1U} = \rho_1 |h_4|^2 / d_1^m \quad (13)$$

In the third time slot, R transmits signals to UE2 and S to assist in completing the information exchange between S and UE2. Assuming that all the energy harvested by R in the first two slots is used for signal transmission in the third time slot, the transmit power of R in the third time slot can be expressed as:

$$\begin{aligned} P_R &= \frac{E_1 + E_2}{(1-2\theta)T} \\ &= \frac{\theta \eta \beta}{(1-2\theta)T} \left(\frac{P_S}{d_2^m} |h_2|^2 + \frac{P_2}{d_3^m} |h_3|^2 \right) \\ &= a |h_2|^2 + b |h_3|^2 \end{aligned} \quad (14)$$

$$\text{where } a = \frac{\theta \eta \beta}{(1-2\theta)T} \frac{P_S}{d_2^m}, \quad b = \frac{\theta \eta \beta}{(1-2\theta)T} \frac{P_2}{d_3^m}.$$

In the third time slot, the relay R uses the collected energy to broadcast a normalized signal $x_R = b_1 x_2 + b_2 x_{2U}$ to both S and UE2, where $b_1 + b_2 = 1$ is the static power allocation ratio, which determines how the relay allocates power to the decoded signal based on the statistical CSI (or statistical channel gain). The relay R decodes the signal and

forwards it to UE2 and S. Since both UE2 and S have their own priori information that can be subtracted from the received signal, the signal received by UE2 and S can be expressed as:

$$y_{UE2}^3 = \sqrt{\frac{P_R}{d_3^m}} h_6 b_1 x_2 + n_2 \quad (15)$$

$$y_S^3 = \sqrt{\frac{P_R}{d_2^m}} h_5 b_2 x_{2U} + n_S \quad (16)$$

The SNR for S decoding x_{2U} is:

$$\gamma_{S,x2U} = b_2 \rho_R |h_5|^2 / d_2^m \quad (17)$$

The SNR for UE2 decoding x_2 is

$$\gamma_{2,x2} = b_1 \rho_R |h_6|^2 / d_3^m, \text{ where } \rho_R = P_R / N_0 \quad (18)$$

3. Results and discussion

3.1. Outage probability analysis

In this section, we derive expressions for the outage probability of the SWIPT-based TWR NOMA system over Rayleigh fading channels. The OP is defined as the probability that the effective end-to-end SINR at the receiver node drops below a certain threshold due to channel fading or interference, and is denoted by P_{out} below.

3.1.1. Outage probability of UE 1

The OP of UE 1 can be expressed as:

$$P_{out}^{UE1} = 1 - P_r(\gamma_{UE1,x2} > \gamma_2, \gamma_{UE1,x1} > \gamma_1, \gamma_{S,x1U} > \gamma_1) \quad (19)$$

Where $\gamma_1 = 2^{2R_1} - 1$, $\gamma_2 = 2^{2R_2} - 1$, R_1 and R_2 is the target data rate for detecting signals for UE1 and UE2, respectively.

Put formulas (4), (5), and (12) into formula (18), the OP of UE1 can be written as

$$P_{out}^{UE1} = 1 - P_r \left(\begin{aligned} &\gamma_{UE1,x2} = \frac{\rho_S |h_1|^2 a_2}{\rho_S |h_1|^2 a_1 + d_1^m} > \gamma_2, \gamma_{UE1,x1} = \frac{\rho_S |h_1|^2 a_1}{d_1^m} > \gamma_1 \\ &\gamma_{S,x1U} = \frac{\rho_1 |h_4|^2}{d_1^m} > \gamma_1 \end{aligned} \right) \quad (20)$$

$$= 1 - P_r \left(|h_1|^2 > \max \left(\frac{\gamma_2 d_1^m}{\rho_S (a_2 - a_1 \gamma_1)}, \frac{\gamma_1 d_1^m}{\rho_S a_1} \right) \right) P_r \left(|h_4|^2 > \frac{\gamma_1 d_1^m}{\rho_1} \right)$$

when $(a_2 - a_1 \gamma_1) > a_1$,

$$P_{out}^{UE1} = 1 - P_r \left(|h_1|^2 > \frac{\gamma_1 d_1^m}{\rho_S a_1} \right) \cdot P_r \left(|h_4|^2 > \frac{\gamma_1 d_1^m}{\rho_1} \right) \quad (21)$$

$$= 1 - \int_{\frac{\gamma_1 d_1^m}{\rho_S a_1}}^{\infty} \lambda_1 e^{-\lambda_1 x} dx \cdot \int_{\frac{\gamma_1 d_1^m}{\rho_1}}^{\infty} \lambda_4 e^{-\lambda_4 y} dy$$

$$= 1 - e^{-\frac{\lambda_1 \gamma_1 d_1^m}{a_1 \rho_S} - \frac{\lambda_4 \gamma_1 d_1^m}{\rho_1}}$$

When $(a_2 - a_1 \gamma_1) < a_1$,

$$P_{out}^{UE1} = 1 - e^{-\frac{\lambda_1 \gamma_1 d_1^m}{(a_2 - a_1 \gamma_1) \rho_S} - \frac{\lambda_4 \gamma_1 d_1^m}{\rho_1}} \quad (22)$$

3.1.2. Outage probability of UE 2

In a similar way, the OP of UE2 can be derived. UE2 occurs an outage at the moment of both the relay decoding the signals of S & UE2 unsuccessfully, and S & UE2 decoding the exchanged signals unsuccessfully, thus the OP of UE2 can be expressed as:

$$P_{out}^{UE2} = 1 - P_r \left(\begin{aligned} &\gamma_{R,x2} > \gamma_2, \gamma_{R,x2U} > \gamma_2 \\ &\gamma_{2,x2} > \gamma_2, \gamma_{S,x2U} > \gamma_2 \end{aligned} \right) \quad (23)$$

Put formulas (8), (11), (17), (18) into the above formula, the OP of UE2 can be written as:

$$P_{out}^{UE2} = 1 - P_r \left(\begin{aligned} &\frac{(1-\beta)a_2 \rho_S |h_2|^2}{(1-\beta)a_1 \rho_S |h_2|^2 + d_2^m} > \gamma_2, \frac{(1-\beta)\rho_2 |h_3|^2}{d_3^m} > \gamma_2 \\ &\frac{b_2 \rho_R |h_5|^2}{d_2^m} > \gamma_2, \frac{b_1 \rho_R |h_6|^2}{d_3^m} > \gamma_2 \end{aligned} \right) \quad (24)$$

$$= 1 - P_r \left(\begin{aligned} &|h_2|^2 > \frac{\gamma_2 d_2^m}{(1-\beta)\rho_S (a_2 - a_1 \gamma_2)}, |h_3|^2 > \frac{\gamma_2 d_3^m}{(1-\beta)\rho_2} \\ &|h_5|^2 > \frac{\gamma_2 d_2^m}{b_2 \rho_R}, |h_6|^2 > \frac{\gamma_2 d_3^m}{b_1 \rho_R} \end{aligned} \right)$$

where $|h_2|^2$ and $|h_3|^2$ are the exponential random variables parameters of λ_2 and λ_3 respectively. Let $z = a|h_2|^2 + b|h_3|^2$, the probability density function (PDF) of z can be written as:

$$f(z) = \begin{cases} \frac{\lambda_2 \lambda_3}{a \lambda_3 - b \lambda_2} \left(e^{-\frac{\lambda_2}{a} z} - e^{-\frac{\lambda_3}{b} z} \right) & a \lambda_3 \neq b \lambda_2 \\ \frac{\lambda_2 \lambda_3}{ab} e^{-\frac{\lambda_3}{b} z} & a \lambda_3 = b \lambda_2 \end{cases} \quad (25)$$

When $a \lambda_3 \neq b \lambda_2$ the OP of UE2 is as following:

$$\begin{aligned}
P_{out}^{UE2} &= 1 - \left(\int_0^\infty \frac{\gamma_2 d_2^m}{(1-\beta)\rho_1(a_2-a_1\gamma_2)} \lambda_2 e^{-\lambda_2 x} dx \cdot \int_0^\infty \frac{\gamma_2 d_2^m}{(1-\beta)\rho_2} \lambda_3 e^{-\lambda_3 y} dy \right) \\
&\quad \cdot \int_0^\infty e^{-\frac{\lambda_2 \gamma_2 d_2^m}{b_2 z}} f(z) dz \cdot \int_0^\infty e^{-\frac{\lambda_6 \gamma_2 d_3^m}{b_1 z}} f(z) dz \\
&= 1 - e^{-\frac{\lambda_2 \gamma_2 d_2^m}{(1-\beta)\rho_1(a_2-a_1\gamma_2)} \frac{\lambda_3 \gamma_2 d_3^m}{(1-\beta)\rho_2}} \cdot \left(\frac{\lambda_2 \lambda_3}{a \lambda_3 - b \lambda_2} \right)^2 \\
&\quad \times \underbrace{\int_0^\infty e^{-\frac{\lambda_2 \gamma_2 d_2^m}{b_2 z} - \frac{\lambda_2 z}{a}} dz - \int_0^\infty e^{-\frac{\lambda_6 \gamma_2 d_3^m}{b_2 z} - \frac{\lambda_3 z}{a}} dz}_{I_1} \\
&\quad \times \underbrace{\int_0^\infty e^{-\frac{\lambda_6 \gamma_2 d_3^m}{b_1 z} - \frac{\lambda_2 z}{a}} dz - \int_0^\infty e^{-\frac{\lambda_6 \gamma_2 d_3^m}{b_1 z} - \frac{\lambda_3 z}{a}} dz}_{I_2}
\end{aligned} \tag{26}$$

Using $\int_0^\infty e^{-\frac{\beta}{4x} - \gamma x} dx = \sqrt{\frac{\beta}{\gamma}} K_1(\sqrt{\beta\gamma})$, we have

$$\begin{aligned}
I_1 &= 2\sqrt{\frac{\lambda_5 \gamma_2 d_2^m a}{b_2 \lambda_2}} K_1 \left(2\sqrt{\frac{\lambda_5 \lambda_2 \gamma_2 d_2^m}{ab_2}} \right) \\
&\quad - 2\sqrt{\frac{\lambda_5 \gamma_2 d_2^m b}{b_2 \lambda_3}} K_1 \left(2\sqrt{\frac{\lambda_5 \lambda_3 \gamma_2 d_2^m}{bb_2}} \right)
\end{aligned} \tag{27}$$

$$\begin{aligned}
I_2 &= 2\sqrt{\frac{\lambda_6 \gamma_2 d_3^m a}{b_1 \lambda_2}} K_1 \left(2\sqrt{\frac{\lambda_6 \lambda_2 \gamma_2 d_3^m}{ab_1}} \right) \\
&\quad - 2\sqrt{\frac{\lambda_6 \gamma_2 d_3^m b}{b_1 \lambda_3}} K_1 \left(2\sqrt{\frac{\lambda_6 \lambda_3 \gamma_2 d_3^m}{bb_1}} \right)
\end{aligned} \tag{28}$$

Put formulas (27), (28) into formula (26), so when $a\lambda_3 \neq b\lambda_2$. The OP of UE2 is:

$$P_{out}^{UE2} = 1 - e^{-\frac{\lambda_2 \gamma_2 d_2^m}{(1-\beta)\rho_1(a_2-a_1\gamma_2)} \frac{\lambda_3 \gamma_2 d_3^m}{(1-\beta)\rho_2}} \cdot \left(\frac{2\lambda_2 \lambda_3}{a\lambda_3 - b\lambda_2} \right)^2 I_1 I_2 \tag{29}$$

When $a\lambda_3 = b\lambda_2$. The OP of UE2 is:

$$\begin{aligned}
P_{out}^{UE2} &= 1 - e^{-\frac{\lambda_2 \gamma_2 d_2^m}{(1-\beta)\rho_1(a_2-a_1\gamma_2)} \frac{\lambda_3 \gamma_2 d_3^m}{(1-\beta)\rho_2}} \\
&\quad \times \int_0^\infty e^{-\frac{\lambda_2 \gamma_2 d_2^m}{b_2 z}} \underbrace{\frac{\lambda_2 \lambda_3}{ab}}_{I_3} e^{-\frac{\lambda_3 z}{b}} z dz \\
&\quad \times \int_0^\infty e^{-\frac{\lambda_6 \gamma_2 d_3^m}{b_1 z}} \underbrace{\frac{\lambda_2 \lambda_3}{ab}}_{I_4} e^{-\frac{\lambda_3 z}{b}} z dz
\end{aligned} \tag{30}$$

$$I_3 = 2\frac{\lambda_2 \lambda_2 \gamma_2 d_2^m}{ab_2} K_2 \left(2\sqrt{\frac{\lambda_2 \lambda_3 \gamma_2 d_2^m}{bb_2}} \right) \tag{31}$$

$$I_4 = 2\frac{\lambda_6 \lambda_2 \gamma_2 d_3^m}{ab_1} K_2 \left(2\sqrt{\frac{\lambda_6 \lambda_3 \gamma_2 d_3^m}{bb_1}} \right) \tag{32}$$

Put formulas (31), (32) into formula (30), when $a\lambda_3 = b\lambda_2$, the OP of UE2 is

$$P_{out}^{UE2} = 1 - e^{-\frac{\lambda_2 \gamma_2 d_2^m}{(1-\beta)\rho_1(a_2-a_1\gamma_2)} \frac{\lambda_3 \gamma_2 d_3^m}{(1-\beta)\rho_2}} I_3 I_4 \tag{33}$$

3.2. Numerical Results

In this section, we present the numerical results to validate our analytical results derived in the previous section through Monte Carlo simulations. The simulation channel adopts Rayleigh fading channel. The simulation channel adopts Rayleigh fading channel. Main simulation parameters are listed in Table II.

Table 2. Simulation parameters

| Parameter | Value |
|--|-----------------|
| λ_1, λ_4 | 1 |
| $\lambda_2, \lambda_3, \lambda_5, \lambda_6$ | 0.5 |
| noise variance N_0 | 0dB |
| a_1, a_2 | 0.2, 0.8 |
| b_1, b_2 | 0.5 |
| η | 0.8 |
| R_1 and R_2 | 0.5bit / s / Hz |
| $d_1 = d_2$ | 0.3m |
| d_3 | 0.7m |
| path loss index m | 2.7 |

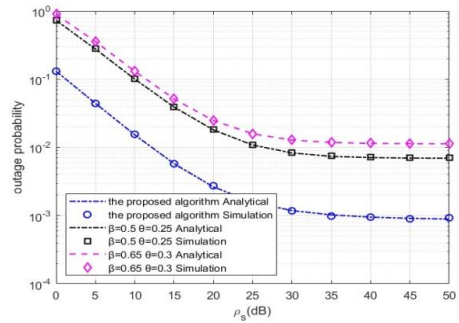


Figure 3. Variation of OP vs ρ_s

Fig. 3 reflects the effect of transmit power on the system outage performance. The optimal β and θ obtained in this paper are compared with the OP performance with baseline scheme 1 and 2. Firstly, the

simulation results verify the correctness of the derived formula. From the figure, it can be seen that the optimal OP for the three cases decreases with the increase of transmit power. Among them, the curves of the outage probabilities for the two baseline schemes are very close. It indicates that optimizing only the time distribution factor or the power distribution factor has a very similar effect on the system outage performance. It implies that the system performance can be greatly improved by jointly optimizing the time switching factor and the power allocation factor.

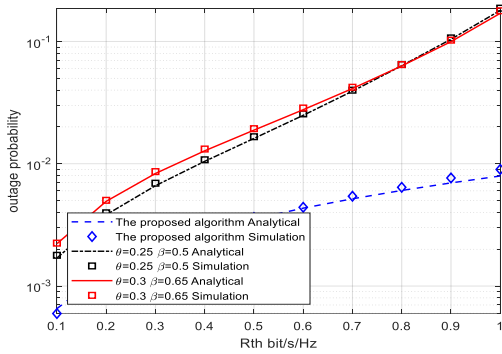


Figure 4. Variation of OP with R_{th} under different schemes

The relationship between the system outage performance and the rate threshold are shown in Fig. 4. It can be seen that the system OP increases with the increase of the rate threshold. It is because when the user's reachable rate threshold increases, the probability of the signal transmission rate less than the rate threshold increases. Thus, the outage performance degrades. The outage performance of the proposed algorithm consistently outperforms the baseline schemes. Therefore, it is possible to make the channel transmit more information with a lower OP by rationally choosing the time allocation factor θ and the power allocation factor β .

Fig. 5 depicts the variation of the system outage performance for the relay position under three scenarios. It can be seen from the figure that the numerical results are in good

agreement with the simulation results. Due to the effect of channel fading, the system OP increases initially and then decreases with d_2 increase. Compared with baseline schemes, the performance of the proposed algorithm is optimal when $d_2 = 0.5$. This is because when $d_2 = 0.5$, the system is symmetric and the transmit power of the relay is equally distributed. So the performance is optimal.

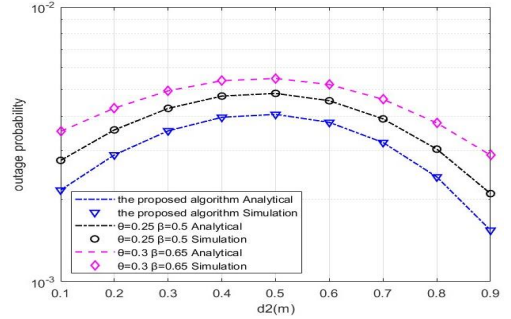


Figure 5. Variation of OP with S-R distance for different schemes

Fig. 6 depicts the variation of the system outage performance with respect to the energy harvesting efficiency η under three scenarios. Energy harvesting efficiency η refers to the receiver's effectiveness in converting the collected energy into electrical energy. As η increases, relays can collect more energy to improve outage performance. It can be observed from Fig. 6 that the OP of the system gradually decreases with η increase. In addition, the outage performance of the proposed algorithm is better than that of baseline schemes.

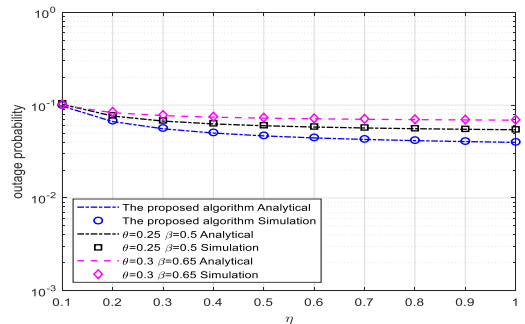


Figure 6. Variation of OP with η for different schemes

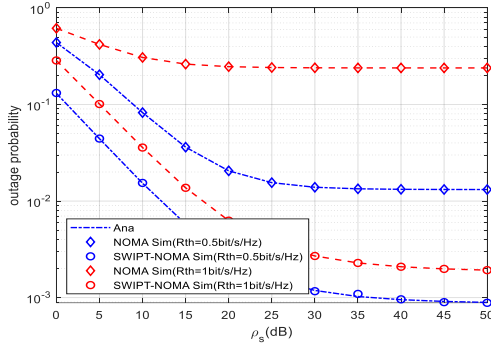


Figure 7. Variation of OP with P_s under different transmission modes

Fig. 7 gives the variation of system outage performance with transmit power for the two transmission modes which contains NOMA and SWIPT-NOMA in this paper at different the rate threshold. It can be seen from Figure 8 that when transmit power increases, the OP of both transmission modes decreases. The OP increases with the increase of the rate threshold. Under a fixed he rate threshold, the proposed algorithm has lower system OP compared with NOMA scheme in [10], where the relay does not have energy harvesting function. In contrast, the scheme proposed in this paper uses energy harvesting relays with dynamic time and power factor optimization algorithms. Thus, it proves that the combination of SWIPT and NOMA can obtain more transmission energy and thus achieve better outage performance.

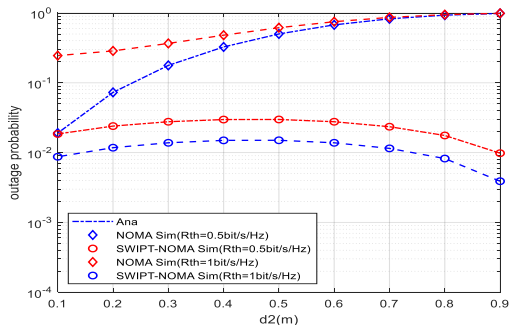


Figure 8. Variation of system OP with relay location for different transmission modes

Fig. 8 gives the variation of the outage performance of the system with the location of the relay in different transmission modes.

It can be seen that the outage performance of the SWIPT-NOMA system in this paper is better than that of NOMA transmission in [10] regardless of the location of the relay. This is because, as the distance between S and R increases, the channel quality between S and R becomes worse, resulting in a smaller strength of the received signal from R and an increase in OP. In contrast, for TWR networks with energy harvesting, more energy is harvested and the transmission performance is better when R is close to either S or UE2. Therefore, the optimal location of the two-way energy-carrying relay should be close to either S or UE2.

4. Conclusion

In this paper, a SWIPT-enabled TWR integrated with the infrastructure based NOMA network over Rayleigh fading channels is considered. We propose a three-phase data exchange scheme based on hybrid relaying protocol combining PS with TS protocol (HPTSR). The closed expressions of OP for the near user and the far user are derived. To achieve a lower system OP under the constraints of power allocation factor and time allocation factor, an iterative algorithm is proposed. Our simulation results outperform baseline scenarios. In the future, we shall extend our work to capture a scenario where reconfigurable intelligent surface (RIS) assisted TWR NOMA network will be considered.

References

1. B. Zheng, X. Wang, M. Wen and F. Chen, "NOMA-Based Multi-Pair Two-Way Relay Networks With Rate Splitting and Group Decoding," in IEEE Journal on Selected Areas in Communications, vol. 35, no. 10, pp. 2328-2341, Oct. 2017, doi: 10.1109/JSAC.2017.2726008.
2. Y. Xu et al., "Joint Beamforming and Power-Splitting Control in Downlink

- Cooperative SWIPT NOMA Systems*," in IEEE Transactions on Signal Processing, vol. 65, no. 18, pp. 4874-4886, 15 Sept.15, 2017, doi: 10.1109/TSP.2017.2715008.
3. C. Y. Ho and C. Y. Leow, "*Cooperative non-orthogonal multiple access using two-way relay*," 2017 IEEE International Conference on Signal and Image Processing Applications (ICSIPA), Kuching, Malaysia, (2017), pp. 459-463, doi: 10.1109/ICSIPA.2017.8120655.
 4. A. Mukherjee, T. Acharya and M. R. A. Khandaker, "*Outage Analysis for SWIPT-Enabled Two-Way Cognitive Cooperative Communications*," in IEEE Transactions on Vehicular Technology, vol. 67, no. 9, pp. 9032-9036, Sept. 2018, doi: 10.1109/TVT.2018.2840140.
 5. Zaidi S K , Hasan S F , Gui X .Two-way SWIPT-aided hybrid NOMA relaying for out-of-coverage devices[J].Wireless Networks, (2020), 26(3):2255-2270, doi:10.1007/s11276-019-02139-8.
 6. Xu Z , Wang S , Liu D ,et al.Joint beamforming and power-splitting optimization for SWIPT-enabled MISO full-duplex two-way cooperative NOMA systems[J].Physical Communication, 2020,45(1):101257,doi:10.1016/j.phycom.2020.101257.
 7. D. Kumar, P. K. Singya, J. Nebhen and V. Bhatia, "*Performance of SWIPT-Enabled FD TWR Network With Hardware Impairments and Imperfect CSI*," in IEEE Systems Journal, vol. 17, no. 1, pp. 1224-1234, March 2023, doi: 10.1109/JSYST.2022.3183501.
 8. S. Althunibat, H. Hassan, T. Khattab and N. Zorba, "*A New NOMA-Based Two-Way Relaying Scheme*," in IEEE Transactions on Vehicular Technology, vol. 72, no. 9, pp. 12300-12310, Sept. 2023, doi: 10.1109/TVT.2023.
 9. Chun Yeen Ho, Chee Yen Leow, Zhiguo Ding, Two-way relay assisted non-orthogonal multiple access,Computer Communications,Volume 145,2019, Pages 335-344, ISSN 0140-3664, <https://doi.org/10.1016/j.comcom.2019.07.012>.